

6-1-2007

Electrical readouts of single and few molecule systems in metal-molecule-metal device structures

Ajit K. Mahapatro

Birck Nanotechnology Center, School of Electrical and Computer Engineering, Purdue University, ajit@purdue.edu

David B. Janes

Purdue University, david.b.janes.1@purdue.edu

Follow this and additional works at: <http://docs.lib.purdue.edu/nanodocs>

Mahapatro, Ajit K. and Janes, David B., "Electrical readouts of single and few molecule systems in metal-molecule-metal device structures" (2007). *Other Nanotechnology Publications*. Paper 22.

<http://docs.lib.purdue.edu/nanodocs/22>

This document has been made available through Purdue e-Pubs, a service of the Purdue University Libraries. Please contact epubs@purdue.edu for additional information.

Electrical Readouts of Single and Few Molecule Systems in Metal-Molecule-Metal Device Structures

Ajit K. Mahapatro* and David B. Janes

School of Electrical and Computer Engineering, Purdue University, West Lafayette, Indiana-47907, USA

Electrical conduction through molecular junctions are measured in different local environments through two test beds that are ideal for single/few molecule and molecular monolayer systems. A technique has been developed to realize Au films with ~ 1.5 Å surface roughness comparable to the best available techniques and suitable for formation of patterned device structures. The technique utilizes room temperature e-beam evaporated Au films over oxidized Si substrates silanized with (3-mercaptopropyl)trimethoxysilane (MPTMS). The lateral (single/few molecule) and vertical (many molecules) device structures are both enabled by the process for realizing ultraflat Au layer. Lateral metal-molecule-metal (M-M-M) device structures are fabricated by forming pairs of Au electrodes with nanometer separation (nano-gap) through an electromigration-induced break-junction (EIBJ) technique at room temperature and conductivity measurements are carried out for dithiol functionalized single molecules. We have used the flat Au layer (using the current technique) as the bottom contact in vertical M-M-M device structures. Here, molecular self-assembly are formed on the Au surface, and patterned ($20 \times 20 \mu\text{m}^2$) top Au contacts were successfully transferred on to the device using a stamping technique (where the Au is deposited on a polydimethylsiloxane (PDMS) pad and following a physical contact on the thiolated Au layer). The single molecular property of XYL, a highly conductive molecule and many molecular property of HS-C9-SH, an insulating molecule in its molecular monolayer form are measured. Observation of enhanced conduction following molecular deposition, and comparison of conductance–voltage characteristics to those predicted theoretically, confirms the success of trapping single/few molecules in the nano-gap. The observed $\sim 10^2$ less conductance through the molecular monolayer of HS-C9-SH compared to the estimation of a linear sum of single molecule conductances over large area indicate that either all the molecules are not in physical contact with the top stamping electrode or electrode-molecule coupling has a less broadening in presence of its own environment or both.

Keywords: Molecular Junctions, Ultra-Flat Gold Surface, Electromigration, Nanogap, Stamping Technique, Large Area Molecular Devices.

1. INTRODUCTION

Electrical readouts of the single or few organic molecules are of great interest to the nano-science and technology. Generally, the electrical properties of the molecular systems are studied through a metal-molecule-metal (M-M-M) device structure fabricated by sandwiching the test molecules (by self-assembling) between two metal electrodes in lateral or vertical configurations. Lateral device structures (LDSs) are performed by anchoring dithiol functionalized molecules between pairs of metal electrodes in molecular scale gap that are formed using a break junction technique (mechanically controlled^{1,2} or electromigration induced).^{3–7} Whereas, the vertical device

structures (VDSs) are fabricated by approaching a second (or top) electrode towards a molecular monolayer. This is performed through scanning tunneling microscopy (STM),^{8–9} conducting probe atomic force microscopy (C-AFM),¹⁰ cross-wire,¹¹ and top metal contact with drop of liquid mercury¹² and deposition through nanopore techniques.¹³

Among the challenges in realizing well-controlled device structures are the difficulties in achieving Au surfaces with molecular scale roughness in patterned devices and nano-scale gaps between contacts in planar structures. In this work, we have developed a technique for realizing ultraflat Au over oxidized silicon surfaces with a molecular adhesion monolayer of (3-mercaptopropyl)trimethoxysilane (MPTMS) using a procedure that should be compatible with micro-fabricating techniques. We have applied

*Author to whom correspondence should be addressed.

the resulting Au layers in both lateral (few molecule) and vertical (many molecules) molecular electronic device structures. The device structure for single/few molecule experiments are carried out by assembling the dithiol-functionalized molecules between Au electrodes with molecular scale gaps formed through electromigration-induced break junction (EBJ) technique and for molecular monolayer devices, a stamping technique is adopted to form the top Au electrode over the molecular self assembly on ultra-flat Au substrates. This accounts a comparison in electronic properties that are observed for molecular systems consisting of single unit (single molecule systems) and with the presence of its own environment (many molecule systems). The single molecular property of XYL, a highly conductive molecule and many molecular property of HS-C9-SH, an insulating molecule in its molecular monolayer form are measured. Enhanced conduction through the nanogaps after growing a self-assembled monolayer conforms the successful bridging of single/few molecules between the nano-electrodes. It is observed that the alkanedithiol molecules show less conductive in molecular monolayer devices ($\sim 400 \mu\text{m}^2$) compared to that of single molecule devices.

2. EXPERIMENTAL DETAILS AND RESULTS

Generally, gold (Au) is used as a suitable metal surface in molecular characterization for its well ordered molecular self assembly properties and probing molecules for molecular electronics study. However, Au is incompatible with the commonly used oxidized silicon surface and a metallic (Ti or Cr) layer is used to support the Au films by giving a sufficient adhesion between SiO_2 and Au. In our currently used technique, the hydroxyl modified SiO_2 surface was exposed to vapor-phase MPTMS molecules (procured from Aldrich and Co., USA) within the evacuated desiccator and then Au is deposited by e-beam evaporation. The detailed experimental procedure and chemical processes involved are described in our earlier work.¹⁴ In the molecular form, MPTMS ($\text{C}_6\text{H}_{16}\text{O}_3\text{SSi}$) has a three straight carbon chained molecule having silane and thiol groups at the two extremities. The silane group by hydrolysis-condensation reactions, interact with surface silanols of the substrates (vertical condensation), react with themselves to form siloxanes by horizontal condensation to form O-Si-O covalently bonded networking of monolayer over the SiO_2 surface. In addition to the bottom O-Si-O bond, the sulphur-gold (S-Au) bond at the top evaporated Au contact, makes MPTMS an efficient adhesive monolayer between bottom SiO_2 and top evaporated Au film. A schematic diagram showing the Au film over a MPTMS capped SiO_2 substrate is shown in Figure 1(a). The surface morphology of the samples was determined by imaging using a Veeco Dimension 3100 atomic force microscope (AFM) in tapping mode. An AFM image of the gold surface in a $\text{Si/SiO}_2/\text{MPTMS}/\text{Au}(200 \text{ \AA})$ structure is shown

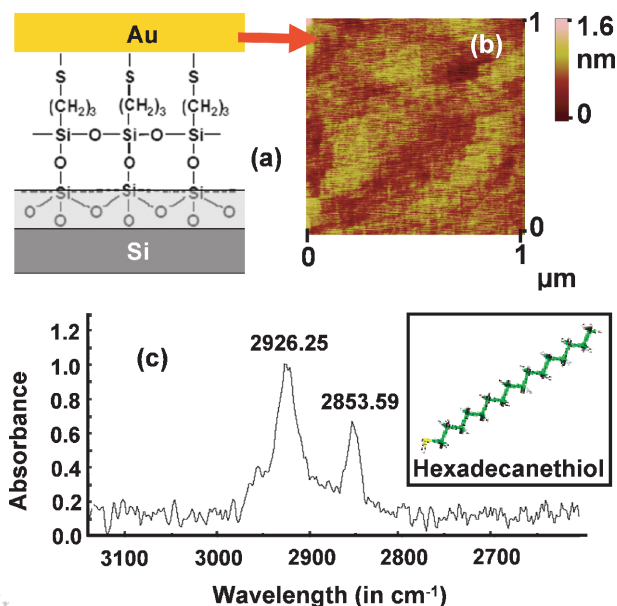


Fig. 1. (a) A schematic of an Au layer deposited over SiO_2 substrate with the molecular adhesion of MPTMS, showing the bottom Si-O-Si covalent and top Au-S chemical bonds. (b) Topography of a 200 Å thick Au layer using the current technique, showing a rms surface roughness of $\sim 1.5 \text{ \AA}$ over $1 \mu\text{m}^2$ area. (c) Transmittance FTIR spectroscopy of 1-hexadecanethiol, which shows a well ordered SAM over the ultra-flat Au surface. Inset shows the schematic of the $\text{C}_{16}\text{-SH}$ molecule.

in Figure 1(b) that shows a rms surface roughness of 1.5 \AA over a scan area of $1 \mu\text{m}^2$. Different studies show a consistent surface roughness of $1.0\text{--}2.0 \text{ \AA}$ for MPTMS/Au samples compared to $6.0\text{--}40 \text{ \AA}$ for Au/Ti samples, each consisting of 20 nm Au films. The above observation indicates that the MPTMS/Au shows a significantly lower surface roughness than that of the Au/Ti sample, with an overall roughness (of $1\text{--}2 \text{ \AA}$) comparable to that of the best available techniques for the formation of ultraflat Au^{15,16} (with surface roughness of $1.0\text{--}3.0 \text{ \AA}$, as observed through template stripping^{15,17} and flame annealing¹⁶ methods).

The advantages of this process include the ease of fabricating the required flat Au surface, the absence of post-evaporation processing and the potential for realizing the flat Au surface in patterned regions. Although Au surfaces with flatness in the same range have been observed through template stripping¹⁵ (also observed for platinum surfaces)¹⁷ and flame-annealing,¹⁶ patterned layers required for most device applications are difficult to achieve with these techniques. In addition, the current technique should result in little Au contamination, which can occur during thermal deposition or flame annealing.¹⁶

The MPTMS/Au layer is physically resistant to commonly used chemicals during surface cleaning and SAM formation (including Toluene, Acetone, Methanol, Ethyl alcohol and Dichloromethane). Various photo-lithographic patterns were also developed using several photoresists. Exposure to the above chemicals leave the Au-layer unaffected (no delamination or crack is observed through high

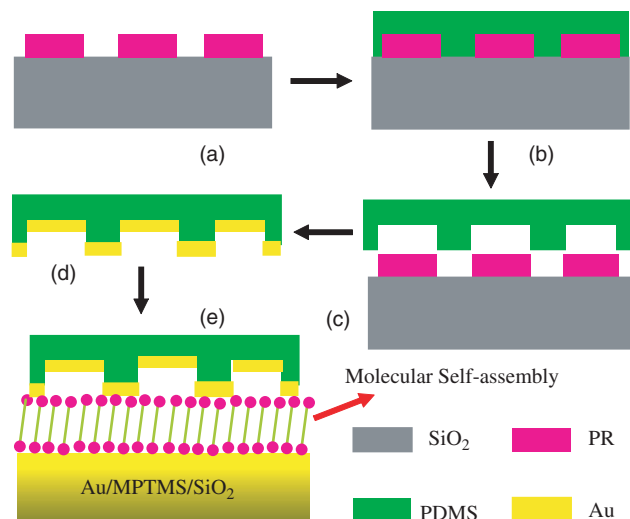


Fig. 2. Schematic of the steps to follow in stamping process: (a) photoresist patterning on SiO_2 substrate, (b) PDMS mold formation, (c) separating the mold (like a rubber stamp) from SiO_2 , (d) Au deposition on the patterned PDMS mold, and (e) making a physical contact over a dithiol modified flat Au surface. Here, the arrows represent the flow of various steps.

resolution microscopy) even after a 30 minute ultrasonification, and exposure to hot plate ($\sim 130^\circ\text{C}$) and UV-light. The physical stability of the Au-layer indicates that the atomically-flat Au surfaces formed in this technique are generally suitable for molecular characterization and device fabrication for electronic applications. To demonstrate of the Si/ SiO_2 /MPTMS/Au structure yields a suitable substrate for formation of well-ordered SAMs, a 1-hexadecanethiol monolayer was deposited by a solution technique (by immersing the Au substrate into a 2 mM solution of C16-SH in ethanol). Figure 1(c) represents the absorbance FTIR spectroscopy of 1-hexadecanethiol SAM formed over the flat Au surface. The clearly defined peaks at wave numbers 2926.25 and 2853.56 cm^{-1} are characteristic vibrational modes for C–H stretches in the C16-alkane chain,¹⁸ indicating the presence of a well ordered SAM over the ultra-flat Au surface.

The physical stability of the Au film over SiO_2 and its suitability for formation of well-ordered organic monolayers indicate that the films are well-suited as substrates for patterned device fabrication in molecular electronics or other devices involving self-assembled monolayers. We have applied the resulting Au layers for fabricating test devices for single/few molecules and molecular monolayer systems. We have used the flat Au layer (using the current technique) as the bottom contact in vertical M-M-M device structures. A -dithiol functionalized molecule is self assembled on the Au surface, and a patterned ($20 \times 20\text{ }\mu\text{m}^2$) top Au contacts were successfully transferred on to the device using a stamping technique, where the Au is deposited on a patterned PDMS pad and make a physical contact on the thiolated Au layer. Figure 2 illustrates the chemical procedure that was followed during stamping. In

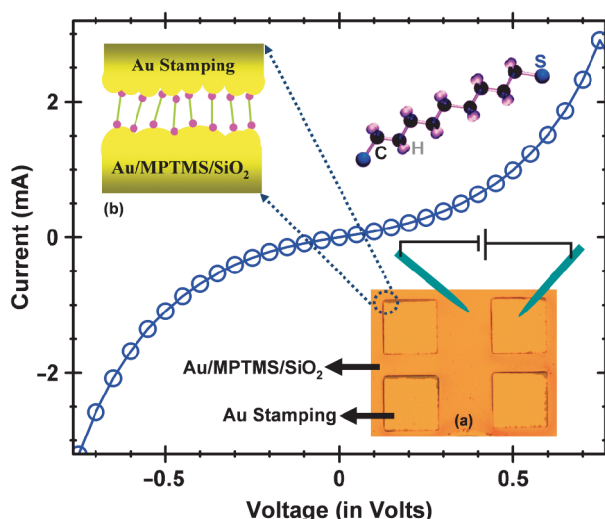


Fig. 3. Room temperature I - V characteristics of Au/C9-dithiol/Au vertical device structure. (a) An Optical microscope image and (b) a schematic view of the M-M-M vertical device structure under study. Inset shows the molecular view of 1,9 nonane-dithiol molecule.

the stamping process, initially the PDMS mold is formed (Fig. 2(b)) over a patterned SiO_2 substrate (Fig. 2(a)) followed by separating the mold from SiO_2 (Fig. 2(c)) and evaporating Au on the PDMS pad (Fig. 2(d)), which then transferred over a molecular self-assembly (Fig. 2(e)).

Electrical conduction through a molecular monolayer is verified by assembling a 1,9 nonane-dithiol monolayer in a VDS configuration illustrated above. Figure 3 shows the non-linear current-voltage characteristic observed through a HS-C₉-SH molecular monolayer by applying a bias to the top (stamped) and bottom MPTMS/Au contacts as demonstrated in Figure 3(a). An optical microscope image of a proto-type device formed using this technique in a Au/HS-C₉-SH/Au structure is shown in Figure 3(a) and the molecular sketch of the resulted device is shown in Figure 3(b). The current density of $2.5 \times 10^5\text{ A/cm}^2$ is observed in devices with a $20 \times 20\text{ }\mu\text{m}^2$ contact area. This value is comparable to the reported value of $3\text{--}6 \times 10^5\text{ A/cm}^2$ for alkanedithiol molecules that are measured in M-M-M structures¹⁹ with evaporated top contacts with device dimension below 100 nm in order to avoid shorts²⁰ (between top and bottom Au).

Pair of electrodes in molecular scale gap is required to probe a single molecule. We have achieved the nano-gaps using an EBJ technique, where a linearly varied voltage bias is allowed to ramped across the Au micro-wires in steps of 20 mV at a rate of 0.25 sec/step. At a threshold voltage V_{th} (corresponding current density J_{th}), $\sim 10^7$ order decrease in current due to the formation of a gap is observed, where Ohmic current through the Au micro-wires change to tunneling current through the nano-gap created between two newly formed Au electrodes. Field emission scanning electron microscope (FESEM) image of a representative nano-gap is shown in Figure 4(a) and

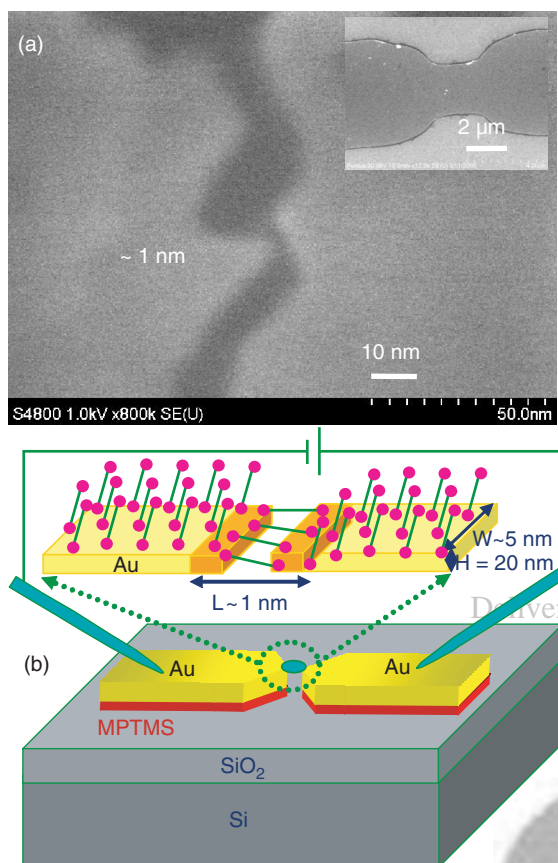


Fig. 4. (a) Schematic of the M-M-M lateral device structure used for single or few molecule systems. Inset shows the expected molecular bridging across the nano-gap. (b) FESEM Image of an EIBJ that shows a ~ 2 nm gap created between two Au electrodes. Insets show the FESEM image of an unbroken Au wire. Although the Au wires are initially $2 \mu\text{m}$ wide, gap of length ~ 2 nm and width ~ 5 nm is observed after the break.

the Au micro-wire before electromigration is shown in the inset of Figure 4(a). The detailed characterization of nano-gaps through FESEM imaging and current-voltage characteristics is discussed elsewhere.²¹

Electrical conduction in a single/few molecule system is verified through M-M-M device structures in lateral configuration (schematic diagram of the device structure is shown in Fig. 4(b)) formed by bridging a dithiol functionalized molecular self-assembly between Au nano-electrodes. A zoomed view of the single/few molecule system observed at the nano-gap region is sketched in inset of Figure 4(b). Figure 5 represents the I - V characteristics of Au/XYL/Au device at room temperature. An increase in current of $\sim 10^5$ is observed in these devices, compared to the currents through the empty-gap devices. This increase in conductivity is observed only in devices with gaps of ~ 1 – 2 nm, but not in devices with gap larger than 2 nm, as determined from empty-gap conductivity levels and subsequent FESEM imaging. Molecular fine structures are reflected in the dI/dV versus voltage plot (shown in inset of Fig. 4) with a conductance gap of 0.4 V, which is predicted theoretically²² as the distance between the

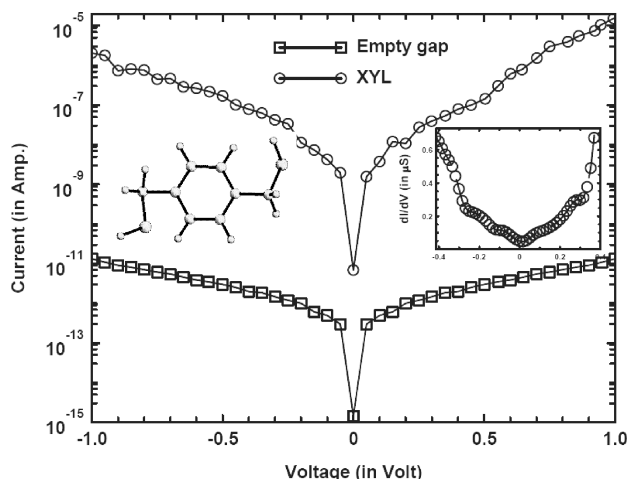


Fig. 5. Room temperature I - V characteristics of Au/XYL/Au (squares) and Au/Empty-gap/Au (circles) device structures. Insets show the molecular formula of XYL (left) and the low bias dI/dV versus the applied voltage.

metal Fermi level and the closest molecular orbital of the molecule at the interface. This molecular signature confirms the presence of molecules between the nanogap and hence the successful bridging of the dithiol molecules of length comparable with the nano-gap between the pairs of Au-nano-electrodes. In another experiment,²³ the suitability of the nano gaps for single/few double stranded (ds)-DNA conductivity studies are verified by measuring the electrical conduction through double-stranded (ds)-DNA molecules, where the dithiol derivatized ds-DNA configuration was immobilized between the EIBJ created Au nano-electrodes. Here, the number of ds-DNA molecules bridging the nano-gap is estimated by comparing the active area of DNA dimension at the break-junction site (as viewed through FESEM) and the surface coverage of the ds-DNA molecules on Au surface (as recorded through quartz crystal microbalance).

Comparison of the single molecule conduction in these two test beds will improve understanding the operating principles of the newly growing molecular devices in electronic circuitry. For molecular junctions with single/few molecule systems, the exact number of molecules that are bridged across the nano-electrodes can not be predicted accurately. This issue has been resolved statistically by considering that the measured conduction is a linear sum of the single molecular events and a normalization procedure^{24–26} is followed to achieve the single molecule conductance. Although, the molecules in molecular monolayer systems are chemically coupled to the electrodes in a same fashion as the single/few molecule systems through Au-S bonding, they may have different physics involved in both the structures because of the presence of surrounding molecules (that may affect the metal-molecule coupling) and different interface properties due to large area contact electrodes. The conduction through a molecule in its own environment is still under study due to lack of

a means to hold the molecules between two electrodes of such large area with a fair electrode-molecule contact. Our current method¹⁴ explores the device dimension over $100\ \mu\text{m}^2$. It is believed that the density of molecules in a molecular monolayer formed over Au surface is about 4.6 molecules/ nm^2 . Our experiment estimates a conductivity of $5.4 \times 10^{-10}\ \text{S/molecule}$ for a system consisting of molecular monolayer of HS-(CH₂)₉-SH, which is two order less than the observed conductivity of $\sim 10^{-8}\ \text{S/molecule}$ that were measured using different techniques.^{26,27} The probable reason for decrease in conductivity may be due to an improper physical contact of the top stamping electrode to all the molecules throughout the device area. Here the effect of electrostatic potential and thermal fluctuation may also have a significant role in decreasing the conductivity²⁸ of the molecule in device dimensions over $\sim 100\ \text{nm}^2$ area.

3. CONCLUSION

To achieve the atomically flat Au surfaces, the hydroxyl modified SiO₂ substrates were silanized with MPTMS and then Au was e-beam evaporated at room temperature. The resulting ultra-flat Au layers remain physically unaffected (as viewed through an optical microscope) by various chemicals and chemical processing during photolithography and self-assembly. The lateral (single/few molecule systems) and vertical (many molecule systems) device structures are both enabled by the process for realizing ultraflat Au layer. The availability of two molecular test beds provides the ability to compare molecular conduction properties in different local environments. The demonstration of 100% yield in fabricating vertical M-M-M device structures using the ultra-flat Au layer illustrates the suitability of the films as substrates in applications to future molecular electronics, where single molecule property can be achieved over large area ($\sim 400\ \mu\text{m}^2$, photo-lithographic scale). The observed $\sim 10^2$ less conductance through the molecular monolayer of HS-C9-SH compared to the estimation of a linear sum of single molecule conductances over large area indicate that either all the molecules are not in physical contact with the top stamping electrode or electrode-molecule coupling has a less broadening in presence of its own environment or both. The current study encourages to study the electrical conduction through molecular junctions that can be efficiently used in future molecular electronics and nano-technology.

Acknowledgments: This work is financially supported by NASA under grant NCC 2-1363 and the NIH Molecular Biophysics predoctoral training grant (T32-GM008296).

References and Notes

1. M. A. Reed, C. Zhou, C. J. Muller, T. P. Burgin, and J. M. Tour, *Science* **278**, 252 (1997).
2. C. Kergueris, J. P. Bourgoin, S. Palacin, D. Esteve, C. Urbina, M. Magoga, and C. Joachim, *Phys. Rev. B* **59**, 12505 (1999).
3. W. Linag, M. P. Shores, M. Bockrath, J. R. Long, and H. Park, *Nature* **417**, 725 (2002).
4. J. Park, A. N. Pasupathy, J. I. Goldsmith, C. Chang, Y. Yaish, J. R. Petta, M. Rinkoski, J. P. Sethna, H. D. Abruna, P. L. McEuen, and D. C. Ralph, *Nature* **417**, 722 (2002).
5. L. H. Yu and D. Natelson, *Nano Lett.* **0**, A (2000).
6. K. I. Bolotin, F. Kuemmeth, A. N. Pasupathy, and D. C. Ralph, *Appl. Phys. Lett.* **84**, 3154 (2004).
7. H. Park, A. K. L. Lim, A. P. Alivisatos, J. Park, and P. L. McEuen, *Appl. Phys. Lett.* **75**, 301 (1999).
8. S. Datta, W. Tian, S. Hong, R. Reifenberger, J. I. Henderson, and C. P. Kubiak, *Phys. Rev. Lett.* **79**, 2530 (1997).
9. E. G. Emberly and G. Kirczenow, *Phys. Rev. Lett.* **91**, 188301 (2003).
10. D. J. Wold and C. D. Frisbie, *J. Am. Chem. Soc.* **123**, 5549 (2001).
11. J. G. Kushmerick, D. B. Holt, J. C. Yang, J. Naciri, M. H. Moore, and R. Shashidhar, *Phys. Rev. Lett.* **89**, 086802 (2002).
12. R. E. Holmlin, R. Haag, M. L. Chabinyc, R. F. Ismagilov, A. E. Cohen, A. Terfort, M. A. Rampi, and G. M. Whitesides, *J. Am. Chem. Soc.* **123**, 5075 (2001).
13. C. Zhou, M. R. Deshpande, M. Reed, L. Jones II, and J. M. Tour, *Appl. Phys. Lett.* **71**, 611 (1997).
14. A. K. Mahapatro, A. Scott, A. Manning, and D. B. Janes, *Appl. Phys. Lett.* (2006), in press.
15. M. Hegner, P. Wagner, and G. Semena, *Surf. Sci.* **291**, 39 (1993).
16. C. Masens, J. Schulte, M. Phillips, and S. Dligatch, *Microsc. Microanal.* **6**, 113 (2000).
17. J. J. Blackstock, Z. Li, M. R. Freeman, and D. R. Stewart, *Surf. Sci.* **546**, 87 (2003).
18. S. H. Brewer, D. A. Brown, and S. Franzen, *Langmuir* **18**, 6857 (2002).
19. W. Wang, T. Lee, and M. A. Reed, *Introducing Molecular Electronics*, edited by G. Cuniberti, G. Fagas, and K. Richter, Springer-Verlag, Berlin (2005), Chap. 10, p. 13.
20. C. Zhou, M. R. Deshpande, M. Reed, L. Jones II, and J. M. Tour, *Appl. Phys. Lett.* **71**, 611 (1997).
21. A. K. Mahapatro, S. Ghosh, and D. B. Janes, *IEEE, Trans. Nano Tech.* **5**, 232, (2006); A. K. Mahapatro, S. Ghosh, and D. B. Janes, Preprint "cond-mat/0503656" at <<http://arXiv.org>> (2005).
22. S. Datta, *Nanotechnology* **15**, S433 (2004).
23. A. K. Mahapatro, K. J. Jeong, G. U. Lee, and D. B. Janes, Unpublished.
24. X. D. Cui, A. Primak, X. Zarate, J. Tomfohr, O. F. Sankey, A. L. Moore, T. A. Moore, D. Gust, G. Harris, and S. M. Lindsay, *Science* **294**, 571 (2001).
25. S. Ghosh, H. Halimun, A. K. Mahapatro, J. Choi, S. Lodha, and D. Janes, *Appl. Phys. Lett.* **87**, 233509 (2005).
26. J. G. Kushmerick, J. Naciri, J. C. Yang, and R. Shashidhar, *Nano Lett.* **3**, 897, (2003).
27. B. Xu and N. J. Tao, *Science* **301**, 1221 (2003).
28. Y. Selzer, L. Cai, M. A. Cabassi, Y. Yao, J. M. Tour, T. S. Mayer, and D. L. Allara, *Nano Lett.* **5**, 61 (2005).

Received: 18 March 2006. Accepted: 22 July 2006.